Nonlinear Model Predictive Control of a Heavy-Duty Hydraulic Bulldozer Blade

Teemu Mononen
Faculty of Engineering and Natural Sciences
Tampere University
Tampere, Finland
teemu.mononen@tuni.fi

Mohammad M. Aref
Faculty of Engineering and Natural Sciences
Tampere University
Tampere, Finland
m.aref@ieee.org

Jouni Mattila
Faculty of Engineering and Natural Sciences
Tampere University
Tampere, Finland
jouni.mattila@tuni.fi

***Abstract*—In this paper, we present a study on nonlinear model predictive control (NMPC) of a bulldozer blade actuated by hydraulic cylinders. We design the controller in the manipulator joint space to track the desired joint angle trajectory. We specify the desired blade cut edge trajectory in the world reference frame and map it to the joint space. In the mapping, we consider the vehicle body orientation and generate a preview of the desired trajectory for the NMPC by estimating the future orientation based on its current value. We test the performance of our controller in MATLAB Simscape. The results show that the proposed controller tracks the desired world frame position with sub-centimeter accuracy regardless of the vehicle body motion and inclination.**

***Keywords*—predictive control, NMPC, hydraulic manipulator**

I. Introduction

A bulldozer is a heavy-duty mobile construction machine that excavates soil using a hydraulically actuated blade and a propulsion system. The resulting ground profile is created by its blade cutting edge position. Controlling the blade position to match the desired surface contour is a difficult task as the blade moves with the vehicle body as it traverses uneven terrain. The operator must compensate for the vehicle inclination and elevation changes by moving the blade in an appropriate way. In this paper, we propose a model-based automatic controller to have the blade cutting edge follow a desired trajectory while the vehicle body moves and inclines.

Model predictive control (MPC) has been utilized for processes with long time constants in the past as prediction of the controlled system behavior is to be computed in real-time. Nowadays, the method has been applied in control of mechanical systems, where controller sampling time requirement is measured in milliseconds. Due to increased power in real-time processing units, MPC and nonlinear MPC (NMPC) are feasible for use in such systems. For example, a complex nonlinear prediction model is introduced in [1], where a quadruped mobile robot is controlled using a whole-body NMPC. The proposed controller predicts not only the robot dynamics but the ground contact as well. The authors show excellent control results with the online optimization running at around 100 Hz and additional controllers at 250 Hz. In [2], NMPC schemes are studied on a 2-link vertical robot manipulator. They show accurate reference tracking using a nonlinear prediction model of the studied system. In [3], the authors propose a combination of feedback linearization and MPC. In doing this, they reduce the complexity of the prediction model vastly and achieve tracking errors of less than 5 mm using 10 ms sampling time.

Hydraulic manipulator systems have highly nonlinear internal dynamics that cannot be neglected in high-precision control design [4]. Flow, friction and valve dynamics often have nonlinear or discontinuous characteristics. For such systems, nonlinear controllers generally produce better control results than linear ones [5]. State-of-the-art model-based control systems for serial and parallel hydraulic manipulators have been reported to reach trajectory tracking errors of less than 5 mm [6]. MPC for such systems was developed in e.g. [7] and [8]. A linear model is used in [7] for general model predictive force control of a hydraulic servo system. Using estimations of the process parameters, the controller produces acceptable results in a variety of experimental tests. In [8], the authors propose an NPMC for a hydraulic forestry crane with an anti-sway feature. They estimate the load sensing hydraulic cylinder dynamics with a discontinuous model and use the manipulator dynamics and kinematics in prediction. Their controller produces acceptable tracking performance with a sampling period of 0.1 seconds with errors ranging from 1.5 cm to 11 cm in experimental tests.

In this paper, we consider a small to medium size bulldozer blade manipulator and propose for it an NPMC control scheme

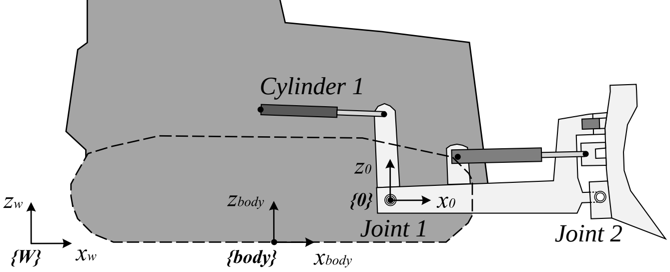

Fig. 1. The studied typical small to medium size bulldozer. The manipulator (light gray) is connected to the body (dark gray) by two connection points at joint 1 position on each side of the machine. The tracks of the machine are see-through in the diagram for clear visualization.

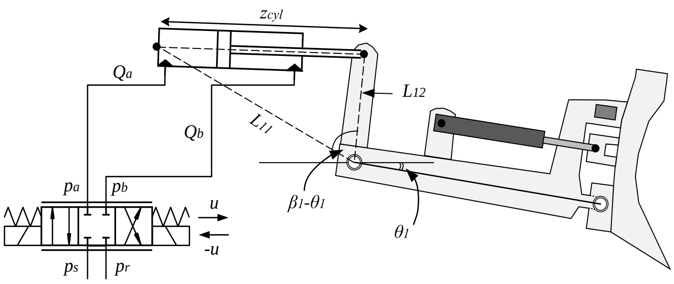

Fig. 2. Joint 1 driven by a hydraulic cylinder. The hydraulic component sizes are exaggerated for visualization. For this diagram, the hydraulic cylinders on each side are lumped as one.

combined with reference signal mapping and previewing. Our control goal is to have the blade follow a specified elevation trajectory in the world coordinate frame while the machine body moves and inclines as the vehicle travels on uneven terrain. We include the dynamics of the hydraulic components and the manipulator in the nonlinear prediction model and compute forward and inverse kinematics outside the online optimization loop. This way, we reduce the computational load of the optimization. As in some systems the used control valves may have characteristics, such as nonlinearities or delays, that make modeling them as constant gains inaccurate, we consider the characteristics of the hydraulic valve in this study.

The rest of this paper is organized as follows. The dynamics of the manipulator system are introduced in Section II. In Section III, we present NMPC for the studied system. Section IV shows the reference signal mapping and previewing algorithm. The proposed control system is tested in simulations and the results are presented in Section V. Finally, Section VI concludes the present study.

II. Dynamics Modeling

A schematic of the studied bulldozer and its blade manipulator is shown in Fig. 1. The manipulator has a revolute joint at its base (joint 1) and a spherical joint at the base of the blade (joint 2). The blade is connected to the manipulator structure that has its connection points to the body on both sides of the machine at joint 1 position (not visible in Fig. 1). There is another cylinder on the opposite side of the vehicle connected to the blade manipulator structure in a similar fashion as cylinder 1. Mounted on the manipulator structure are two more cylinders used for blade heading control and one cylinder for blade roll. We do not consider these cylinders in this study. This manipulator structure is typical for small to medium size bulldozers with one translational and two rotational degrees of freedom (DOF). The vehicle body can incline about three axes as the machine traverses uneven terrain. These rotations are described in the vehicle body fixed frame whose orientation coincides with the world coordinate frame. The body inclination and manipulator are modeled using MATLAB Simscape and the hydraulics using MATLAB Simulink.

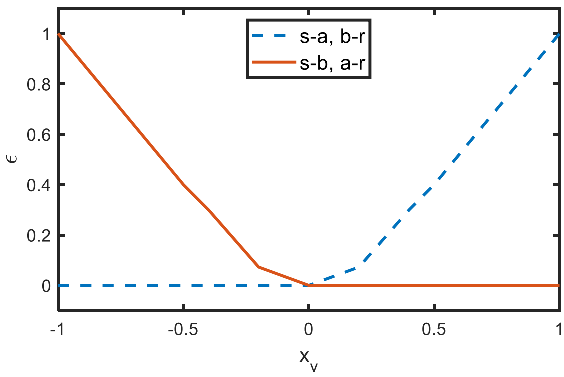

Fig. 3. The nonlinear relation between the valve spool position x_v and the relative flow path opening $\epsilon = Q/Q_{max}$. The flow paths are from supply port (s) to chamber a, supply to chamber b, chamber a to return line (r) and chamber b to return line.

A. Manipulator

The manipulator is illustrated in Fig. 2. In control design, we consider the dynamics of the first joint while assuming that the spherical joint angles are constant. With this assumption, the dynamics of the manipulator can be written as

$$J_b\ddot{\theta}_1 = \tau - mgd\cos(\theta_1) - \tau_{ext} \tag{1}$$

Where J_b is the manipulator moment of inertia, τ is the joint input torque, m is the mass of the manipulator, g is acceleration due to gravity, d is the distance from joint 1 origin to the manipulator center of mass and τ_{ext} is the external torque. Note the $\theta_1 = 0$ position in Fig. 2.

The force produced by the hydraulic cylinders is mapped to joint actuating torque by $\tau = J(\theta)F$, where

$$J = -\frac{L_{11}L_{12}\sin(\beta_1 - \theta_1)}{\sqrt{L_{11}^2 + L_{12}^2 + 2L_{11}L_{12}\cos(\beta_1 - \theta_1)}} \tag{2}$$

The measures and angles are visualized in Fig. 2. The total length of the hydraulic cylinder is determined from the joint angle as

$$z_{cyl} = \sqrt{L_{11}^2 + L_{12}^2 - 2L_{11}L_{12}\cos(\beta_1 - \theta_1)} \tag{3}$$

For brevity, we do not present the kinematics of the manipulator in this paper. We denote the transformation matrix from frame 0 to world reference frame as ${}^{W}_{0}T$, which depends on the machine inclination and joint angles.

B. Hydraulics

The hydraulics consist of a hydraulic valve and two identical cylinders. The flow from the valve is distributed evenly to both cylinders. In Fig. 2, these cylinders are lumped as a single cylinder where the total fluid flow enters. In this study, we consider the dynamics of the hydraulic valve, that have an effect on the system behavior. The dynamics of the valve spool motion are expressed using a second order linear model

$$\ddot{x}_v = -2\xi\omega_n\dot{x}_v - \omega_n^2 x_v + \omega_n^2 u \tag{4}$$

where x_v is the spool position, ξ is the damping term, ω_n is the natural frequency and u the control input. The relation from valve spool position to flow path relative opening ϵ is a nonlinear one described using a lookup table shown in Fig. 3.

The flow rates entering into the cylinder chambers can be expressed as

$$Q_a = K_v v(p_S - p_a)\epsilon S(\epsilon) + K_v v(p_a - p_r)\epsilon S(-\epsilon) \quad (5)$$

$$Q_b = -K_v v(p_S - p_b)\epsilon S(-\epsilon) - K_v v(p_b - p_r)\epsilon S(\epsilon) \quad (6)$$

Where K_v is the flow coefficient of the valve, p_a and p_b are the cylinder chamber pressures, p_S is the supply pressure, p_r is the return line pressure, $S(\epsilon)$ is a selective function [4]

$$S(\epsilon) \stackrel{\text{def}}{=} \begin{cases} 1, & if\ \epsilon > 0 \\ 0, & if\ \epsilon \le 0 \end{cases} \quad (7)$$

And $v(\Delta p)$ is the following pressure difference function

$$v(\Delta p) = \text{sign}(\Delta p)\sqrt{|\Delta p|} \quad (8)$$

As the flow from the valve is distributed evenly to both cylinders, the pressure dynamics in the cylinder chambers are expressed as

$$\dot{p}_a = \frac{\beta}{A_a x}\left(\frac{Q_a}{2} - A_a\dot{x}\right) \quad (9)$$

$$\dot{p}_b = \frac{\beta}{A_b(x_{max} - x)}\left(\frac{Q_b}{2} + A_b\dot{x}\right) \quad (10)$$

Here, β is the bulk modulus of the fluid, A_a and A_b are the piston areas in both chambers, and x_{max} is the maximum stroke of the cylinder piston. The force produced by the hydraulic cylinder can be written as

$$F = p_a A_a - p_b A_b - F_\mu \quad (11)$$

where F_μ is the cylinder friction modeled using the Stribeck model with viscous friction [9]:

$$F_\mu = \text{sign}(\dot{x})\left(f_c + (f_s - f_c)e^{-\left(\frac{\dot{x}}{v_s}\right)^2}\right) + b_c\dot{x}, \quad (12)$$

where f_c is the Coulomb friction, f_s the static friction, b_c viscous friction coefficient and v_s the Stribeck velocity.

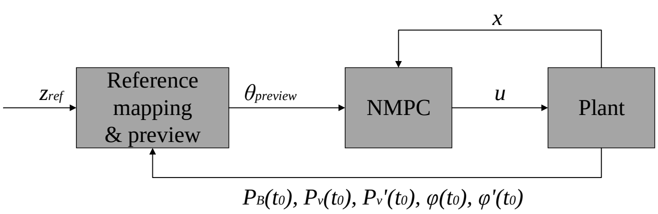

Fig. 4. The proposed control system architecture.

III. Nonlinear Model Predictive Control of the Manipulator

The nonlinear model predictive controller uses a nonlinear dynamic model to predict the future states of the controlled system. We construct this model for the studied manipulator using equations (1)-(12). In this study, the control objective is to follow a desired joint trajectory that corresponds to a desired blade cut edge trajectory in the world reference frame. We design our controller in the manipulator joint space and use a reference trajectory mapping outside the NMPC prediction. This mapping accounts for the vehicle body inclination and position and is described in detail in Section IV. The control system block diagram is shown in Fig. 4. The NMPC problem can be summarized for each sampling time as:

$$\begin{aligned} &\min_{u(\cdot)} J_R(x_k, u_k) \\ s.t. \quad & x_{k+1} = f_d(x_k, u_k) \\ & x(0) = x_0 \\ & u_{min} \le u_k \le u_{max} \\ & x_{min} \le x_k \le x_{max}, \end{aligned} \quad (13)$$

where the current state is set as the initial value x_0, similar to [8] and [10], and $u(\cdot)$ is the optimal control sequence. In this study, we use discrete-time receding horizon NMPC, where a discretized system model f_d based on equations (1)-(12) is used and the first element of $u(\cdot)$ is used for control each sampling instance. The state vector of the nonlinear prediction model is

$$x = [\theta_1 \quad \dot{\theta}_1 \quad p_a \quad p_b \quad x_v \quad \dot{x}_v]^T \quad (14)$$

The control input is the valve input u. To achieve the target joint angle tracking, we include terms penalizing the tracking error and control valve input to the cost function. The cost function in the discrete case at time t_0 is then defined as

$$\begin{aligned} J_R = &\sum_{k=1}^{N_p-1} Q_\theta(k)\left(\theta_{1ref}(t_0 + kT_s) - \theta_1(t_0 + kT_s)\right)^2 \\ &+ \sum_{n=1}^{N_c} R\big(u(t_0 + (n-1)T_s) - u(t_0 + nT_s)\big)^2 \\ &+ W\left(\theta_{1ref}(t_0 + N_pT_s) - \theta_1(t_0 + N_pT_s)\right)^2 \end{aligned} \quad (15)$$

Where $Q_\theta(k)$ and R are the cost coefficients for joint 1 angle error and valve input, respectively, N_p is the length of the prediction horizon and N_c the length of the control horizon. W is the terminal cost penalizing tracking error at the end of prediction horizon. To enhance trajectory tracking performance, we use exponentially increasing weight on the tracking error: $Q_\theta(k) = 2^{k-1}Q$ [11]. The cost J_R is computed for the duration of the prediction horizon. For predictions after the control horizon, the control input is kept constant at $u(t_0 + N_cT_s)$ and the cost function thus only penalizes the angle error. As seen in the cost function, a preview of the reference signal is provided for the duration of the prediction horizon. This feature improves the controller performance when the future reference values are known.

The limits for the control input are based on the valve operation, which restricts the valve opening between the two extremums. I.e. $u \in [-1, 1]$. Restriction on the joint angle is made based on the angles corresponding to the minimum and maximum length of the hydraulic cylinder. In our tests, however, these restrictions are not reached.

IV. Reference Signal Mapping

We assume that a reference trajectory for the blade cutting edge is available in the world reference frame. On a construction site this trajectory is defined in space coordinates rather than time domain. Assuming that the vehicle travels in a straight line, i.e. $\dot{y}_v \equiv 0$, we can map the space trajectory to time domain using the current velocity of the vehicle. Then, for discrete points of the trajectory, we get

$$\Delta t = \Delta x / v \qquad (16)$$

We then map this reference signal to the manipulator joint space based on knowledge of the machine position, pitch angle, angular velocity and the manipulator joint angles. First, we map the desired position in the world frame (${}^{W}P_d$) to frame 0 (${}^{0}P_d$) using the transformation matrix ${}^{0}_{W}T = {}^{W}_{0}T^{-1}$ and then, using inverse kinematics, to the joint space. Note, that the manipulator x and y coordinates in the world frame cannot be controlled by manipulator joint angles but instead the movement of the mobile base. The elevation, i.e. z coordinate, however, can be controlled by means of joint 1 angle.

To create a preview of the reference signal for the NMPC, we need to predict the vehicle body pitch angle φ change for the duration of the prediction horizon. Assuming that the angle is constant throughout the length of the horizon is not an adequate prediction. Thus, we use the pitch angular velocity to create a prediction that is sufficiently accurate for a relatively short prediction horizon. We can use similar prediction for the vehicle motion in the world reference frame. By acquiring the velocities in x, y and z directions, we assume that over the prediction horizon, these values remain constant. This is formulated in (17).

$$\begin{aligned} \varphi(t_0 + kT_s) &= \varphi(t_0 + (k-1)T_s) + T_s\dot{\varphi}(t_0) \\ z_v(t_0 + kT_s) &= z_v(t_0 + (k-1)T_s) + T_s\dot{z}_v(t_0) \\ x_v(t_0 + kT_s) &= x_v(t_0 + (k-1)T_s) + T_s\dot{x}_v(t_0) \end{aligned} \qquad (17)$$

TABLE 1. Pseudo Code For Reference Preview Mapping

1	Receive $P_B(t_0)$, $P_v(t_0), P_v{}'(t_0)$ and $\varphi(t_0), \dot{\varphi}(t_0)$
2	Set $\theta_{preview}$ = **null**
3	**FOR** m = 0:N_p-1
4	Construct ${}^{W}P_d(t_0 + mT_s)$
5	Compute φ, z_v, x_v at $t_0 + mT_s$ using (17)
6	Compute ${}^{0}_{W}T(t_0 + mT_s) = {}^{W}_{0}T^{-1}(t_0 + mT_s)$
7	Compute ${}^{0}P_d(t_0 + mT_s) = {}^{0}_{W}T(t_0 + mT_s){}^{W}P_d$
8	Compute $\theta_{1ref}(m)$ using inverse kinematics
9	Append $\theta_{1ref}(m)$ to $\theta_{preview}$
10	**ENDFOR**
11	Input $\theta_{preview}$ to the NMPC as (13)

To map the reference and construct the preview, we need the current position of the blade cut edge and the vehicle body fixed frame, P_B and P_v, in the world reference frame. Also needed is the inclination angle and angular velocity of the vehicle body and vehicle velocity $P_v{}'$. The reference mapping and previewing procedure done each sampling instance is summarized as pseudo code in TABLE 1. The resulting vector $\theta_{preview}$ contains N_p reference values from $t = t_0$ sampled at T_s rate. In (15), $\theta_{1ref}(t_0 + kT_s) = \theta_{preview}(k)$.

Note that in line 8 of the pseudocode (TABLE 1), the inverse kinematics computation is based on the blade pose at the start of each prediction iteration. We do not specify the pose of the blade in the vehicle body frame when generating the reference preview for a short horizon. The start pose is assumed to be constant throughout the prediction horizon except for its z-coordinate, which is updated by the desired value before computation of the inverse kinematics. For longer predictions or large pose changes, this may deteriorate the accuracy of the mapping towards the end of the horizon. However, the efficacy of this simplification is seen in the simulation results in Section V.

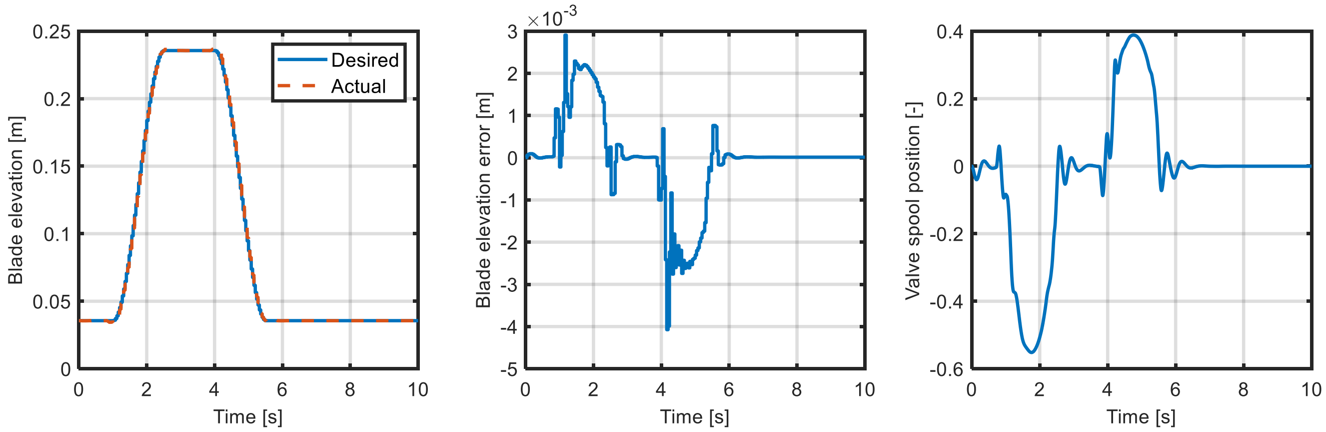

Fig. 5. The simulation results of scenario 1, where the vehicle body is stationary and the blade is driven along a desired trajectory (left). The NMPC weight parameters were $Q = 10, R = 0.0002, W = 50$.

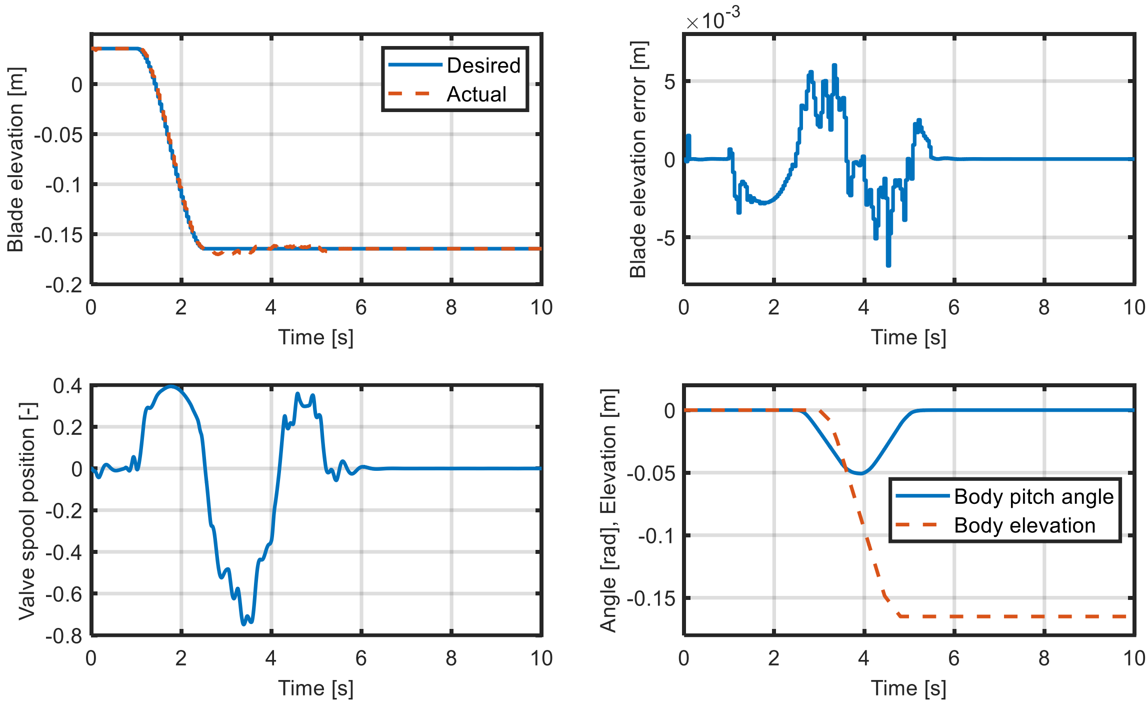

Fig. 6. The simulation results of scenario 2, where the vehicle body is moving in x and z directions and pitching (see bottom right). This scenario represents the blade cutting into soil generating a trench that the vehicle then drives into. The velocity of the vehicle was 1 m/s and the NMPC weight parameters identical to scenario 1.

V. Simulation and Discussion

To test the controller reference tracking performance, we first have the blade move with the mobile base kept stationary in scenario 1. Then, we introduce vehicle body pitch angle and elevation changes to test the proposed linear prediction and mapping in scenario 2. For all the simulation tests, we chose $T_s = 0.04$ s and $N_p = 10, N_c = 5$. The length of prediction is thus 0.4 s. MATLABs fmincon tool is used to solve the online optimization using the SQP algorithm. In the scenarios, we exert no resisting torques on the blade, but show an additional test with a moderate resistance of motion to simulate interactions with ground. For small blade loads, e.g. when finishing a ground surface, the small load torque assumption is valid. For larger resisting forces, a term of the estimated resisting torque, τ_{ext}, can be added to the NMPC prediction model to improve the results.

Fig. 5 illustrates the results from scenario 1. The tracking performance of the controller is excellent when the vehicle body is stationary. The position tracking error is within ±0.004 m throughout the test. Modeling errors and the selected sampling time have an effect on the control performance. The

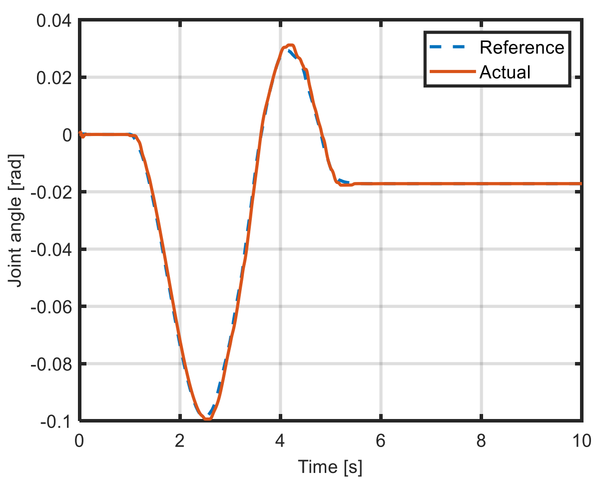

Fig. 7. The reference and actual joint angle during scenario 2 with body motion and inclination (see Fig. 6).

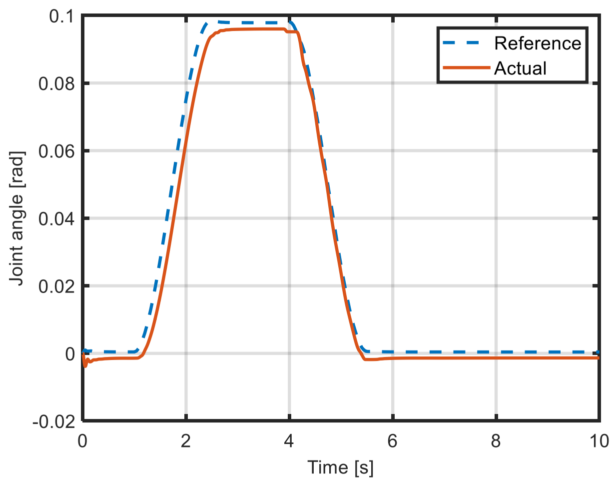

Fig. 8. Joint 1 desired and actual angle in scenario 1 trajectory with downward pulling constant 20 kN external force applied to the blade. The vehicle body was stationary and the NMPC weight parameters identical to scenario 1.

hydraulic control valve is never fully opened to achieve the desired trajectory. This also means that the required cylinder velocity does not exceeded the maximum velocity in this scenario.

Fig. 6 shows the control results when the vehicle body moves in x and z directions, and its pitch angle changes. We generated signals describing these quantities to represent the body motion when the blade cuts a trench to the ground. The vehicle body will incline and descend as the vehicle drives down the created trench. We chose a vehicle travel velocity of 1 m/s for this test. The start of reference tracking is of same quality as in Fig. 5, but as the body starts to incline at 2.5 seconds, the tracking experiences small deterioration. However, despite the vehicle body both inclining and descending, the tracking error is within ±0.007 m throughout the simulation. The simplified reference preview shown in Section IV is effectively generating a reference joint trajectory which cancels out the vehicle body motion effects on blade position tracking. As seen in Fig. 7, the desired joint trajectory tracking has errors, which results in the blade cut edge trajectory errors. The errors are due to the body inclination starting without the controller having any prior knowledge of the fact. The reference previewer does not predict the body motion until it has already started, which causes an initial error at the start of the body motion.

In the final test, a constant 20 kN force was introduced pulling the blade downwards. Fig. 8 illustrates the trajectory tracking scenario seen in Fig. 5 with this added disturbance force. It is clear that the NMPC is unable to follow the desired joint angle trajectory with the unmeasured disturbance force, as the controller receives $\tau_{ext} = 0$ and the system behavior differs from the prediction. We highlight this defect to show where further improvement is required. The bulldozer blade will be in contact with the ground, which will impose resisting forces and thus torques on the joint.

VI. Conclusions

In this paper, we considered the problem of bulldozer blade position control in desired ground contour tracking. Our control goal was blade cut edge trajectory tracking while rejecting the disturbances caused by vehicle body motion We presented a nonlinear model predictive controller with separate reference signal mapping and previewing for a heavy-duty hydraulic bulldozer blade. The proposed controller was designed in joint space, where it tracked the desired joint angle trajectory. As the control end goal, a trajectory specified in the world coordinate frame was to be tracked with the best possible performance by the actuator control in the joint space. We simulated the blade manipulator attached to the vehicle body in MATLAB Simscape. With the proposed control scheme, we obtained reference tracking errors within ±0.007 m with the vehicle body inclining and moving.

We reduced the complexity of the nonlinear prediction model by excluding the forward and inverse kinematics from it. By introducing a separate trajectory mapping and previewing, we could use simplified predictions for the vehicle body inclinations and their effects on the desired joint angle trajectory solved less frequently than the optimization. Blade reference tracking performance can be improved by developing a reference previewer that predicts the vehicle body inclination based on the ground profile cut by the blade. Furthermore, the controller scheme should be developed to include an estimation of the resisting torque so that better control performance in heavy blade loading conditions would be achieved. These aspects are among future research topics.

Acknowledgment

This work was funded by the Doctoral School of Industry Innovations (DSII) of Tampere University.

References

[1] M. Neunert, M. Stäuble, M. Giftthaler, C. D. Bellicoso, J. Carius, C. Gehring, M. Hutter and J. Buchli, "Whole-Body Nonlinear Model Predictive Control Through Contacts for Quadrupeds," *IEEE Robotics and Automation Letters,* vol. 3, no. 3, pp. 1458-1465, 2018.

[2] J. Wilson, M. Charest and R. Dubay, "Non-linear model predictive control schemes with application on a 2 link vertical robot manipulator," *Robotics and Computer-Integrated Manufacturing,* vol. 41, pp. 23-30, 2016.

[3] F. Schnelle and P. Eberhard, "Constraint mapping in a feedback linearization/MPC scheme for trajectory tracking of underactuated multibody systems," *IFAC-PapersOnLine,* vol. 48, no. 23, pp. 446-451, 2015.

[4] J. Koivumäki and J. Mattila, "Stability-Guaranteed Force-Sensorless Contact Force/Motion Control of Heavy-Duty Hydraulic Manipulators," *IEEE Transactions on Robotics,* vol. 31, no. 4, pp. 918-935, 2015.

[5] M. M. Bech, T. O. Andersen, H. C. Pedersen and L. Schmidt, "Experimental evaluation of control strategies for hydraulic servo robot," in *2013 IEEE International Conference on Mechatronics and Automation*, Takamatsu, 2013.

[6] J. Mattila, J. Koivumäki, D. G. Caldwell and C. Semini, "A Survey on Control of Hydraulic Robotic Manipulators With Projection to Future Trends," *IEEE/ASME Transactions on Mechatronics,* vol. 22, no. 2, pp. 669-680, 2017.

[7] G. Wu, N. Sepehri and K. Ziaei, "Design of a hydraulic force control system using a generalized predictive control algorithm," *IEE Proceedings - Control Theory and Applications,* vol. 145, no. 5, pp. 428-436, 1998.

[8] J. Kalmari, J. Backman and A. Visala, "Nonlinear model predictive control of hydraulic forestry crane with automatic sway damping," *Computers and Electronics in Agriculture,* vol. 109, pp. 36-45, 2014.

[9] H. Olsson, K. J. Åström, C. Canudas de Wit, M. Gäfvert and P. Lischinsky, "Friction Models and Friction Compensation," *European Journal of Control,* vol. 4, no. 3, pp. 176-195, 1998.

[10] L. Grüne and J. Pannek, Nonlinear Model Predictive Control: Theory and Algorithms, Springer-Verlag London, 2011.

[11] F. Kühne, J. M. G. da Silva Jr. and W. F. Lages, "Mobile robot trajectory tracking using model predictive control," in *IEEE Latin American Robotics Symposium*, São Luís, 2005.